

POSTLIQUEFACTION DEFORMATION OF COHESIONLESS SOIL

Ashraf K. Hussein and Harry E. Stewart

Graduate Research Assistant and Associate Professor
School of Civil and Environmental Engineering
Cornell University

ABSTRACT

Ground settlements due to reconsolidation of liquefied soils can cause substantial damage to both above ground structures and those buried within the ground. Current methods for predicting the magnitude of settlement rely upon either empirical data collected from a limited number of field sites, or from correlations developed from specialized laboratory tests. Some direct field measurements show that actual settlements can differ significantly from those estimated using the available techniques. Therefore, an understanding of the factors influencing these ground movements is critical for quantifying the magnitude of ground deformations. Constant volume strain-controlled direct simple shear tests at relative densities of approximately 38 and 80% were performed on specimens of Nevada sand. Following liquefaction, an additional 10 to 20 cycles were applied, with shear strains ranging from 0.5 to 15%. The specimens then were allowed to reconsolidate and the volume changes were measured.

Test results indicated that the reconsolidation volumetric strains depended on relative density and initial effective stress. The reconsolidation volume changes were slightly dependent on the shear strain level, up to a shear strain of about 4%, and independent of number of postliquefaction loading cycles. Additional tests were performed in a torsional shear system to confirm the results of the direct simple shear tests. Comparisons of these results with data from other researchers, where reconsolidation strains were found to be related uniquely to the cyclic strains, are discussed in light of design curves used to estimate the magnitude of anticipated ground settlements.

INTRODUCTION

Cyclic ground motion during earthquakes is known to cause volumetric reduction in cohesionless soils, resulting in permanent ground settlement which can cause substantial damage to both above ground structures and those buried within the ground. There are two general mechanisms by which settlements can occur. First, dry cohesionless soils may undergo compaction as a result of repeated shear straining. Mechanisms contributing to settlements of dry soils have been explored and identified by several researchers (Silver and Seed, 1971; Youd, 1972), and analysis methods have been developed to predict settlements in dry soils (Seed and Silver, 1972; Pyke, et al. 1975).

The second general method by which ground settlements develop is related to reconsolidation of saturated deposits as excess pore water pressures generated during undrained cyclic loading are dissipated. Although there are several similarities in the general behavioral aspects of dry and saturated soil settlements, the latter may involve more complex relationships. Simplified and insightful methods for evaluating the anticipated reconsolidation settlements have been proposed, and are very useful for preliminary settlement evaluations. Lee and Albaisa (1974) have proposed methods based on laboratory test results for calculating reconsolidation settlements for situations where the excess pore pressures are less than or just equal to those causing liquefaction. Tokimatsu and Seed (1987) and Ishihara and Yoshimine (1992) have developed more generalized predictive methods that include consideration of not only excess pore pressure dissipation, but also the magnitude of the cyclic shear strain imposed during ground shaking. The importance of including the magnitude of the cyclic shear strains has been demonstrated based on the results of specialized laboratory tests (Ishihara and Yoshimine, 1992; Nagase and Ishihara, 1988; Tatsouka, et al. 1984).

This paper presents the results of a laboratory test program wherein test specimens were liquefied under undrained strain-controlled cyclic loading, subjected to several cycles of straining after initial liquefaction, then allowed to reconsolidate. Constant volume strain-controlled direct simple shear (DSS) tests were performed on a Nevada sand at relative densities, D_r , of approximately 38 and 80%. Following liquefaction, an additional 10 to 20 cycles were applied, with shear strains, γ , ranging from 1 to 15%. The specimens then were allowed to reconsolidate and the volume changes measured. Additional tests were performed in a torsional shear (TS) system for comparison with the results of the direct simple shear tests. Specimen preparation and test procedures are explained, along with test results. Comparisons of these results with data from other researchers, where reconsolidation strains were found to be related uniquely to the cyclic strains, are discussed in light of design curves used to estimate the magnitude of anticipated ground settlements.

TEST PROCEDURES

The tests material in this program was a Nevada sand. The grain size distribution curve for Nevada sand is shown in Figure 1. The sand has a specific gravity of 2.68, and the maximum and minimum void ratios were 0.516 and 0.894, respectively (Arulmoli, et al. (1991)). The NGI direct

simple shear device with wire-reinforced rubber membranes was used in this study to perform constant volume cyclic strain-controlled tests. Sand specimens with a diameter of 66.8 mm and a height of approximately 20 mm were prepared using a dry-tamping method. Specimens were prepared in two layers at relative densities slightly lower than the target densities of approximately 38 and 80% to allow for initial consolidation effects. Although constant volume tests often are done using dry specimens, deaired water was circulated through the specimens under gravity head to minimize concerns about potential water lubrication effects. Each specimen was consolidated to an effective vertical stress of $\bar{\sigma}_{vj} = 54$ kPa or 204 kPa, and the relative density was determined. Then, a constant volume strain-controlled test was conducted using a sinusoidal cyclic strain at frequency of 0.01 Hz until an initial liquefaction condition occurred. The strain amplitudes leading to initial liquefaction were varied over a wide range, up to strain levels wherein liquefaction developed in less than one cycle. Constant volume was achieved using a carefully controlled feedback mechanism throughout testing. After these loadings, the specimen was reconsolidated to the initial effective vertical stress prior to shear, $\bar{\sigma}_{vj}$, and the vertical strain was measured using a linear variable differential transformer. Since tests were conducted using the stiff wire-reinforced membranes, the volumetric reconsolidation strain, ε_v , was equal to the vertical strain.

A series of cyclic undrained strain-controlled tests were conducted using the hybrid resonant column/torsional shear device described by Stewart and Hussein (1992). Solid cylindrical specimens with a height of 193 mm and a diameter of 71 mm were prepared in a split mold using the undercompaction technique developed by Ladd (1978). Specimens were consolidated isotropically at an effective confining pressure of $\bar{\sigma}_{ci} = 150$ kPa. This isotropic consolidation pressure was selected so that the mean effective stress level in the torsional shear tests would be roughly equivalent to that in the DSS tests at $\bar{\sigma}_{vj} = 204$ kPa. After consolidation, undrained strain-controlled cyclic torsional shear tests were performed at shear strain levels ranging from $\gamma_{cy} = 0.1\%$ to 8% until initial liquefaction occurred. Then, the specimens were reconsolidated to the initial effective confining pressure of 150 kPa. The reconsolidation volumetric strain was calculated based on the outflow of pore water and the specimen volume prior to cyclic shear.

TEST RESULTS

The first series of tests was conducted in the DSS device to investigate the effects of cyclic shear strain amplitude, γ_{cy} , relative density, D_r , and initial effective vertical stress, $\bar{\sigma}_{vj}$, on the volumetric strain, ε_v , due to reconsolidation after liquefaction, but without any postliquefaction cyclic straining. After initial liquefaction occurred, specimens were reconsolidated to the initial vertical stress prior to shear of $\bar{\sigma}_{vj} = 54$ kPa or 204 kPa. The average relative densities of the specimens after consolidation were roughly 38 and 80%. The cyclic shear strain amplitude was constant for each test, and ranged from 0.1 to 15%. For shear strain levels greater than about 1%, the specimens sustained less than one complete cycle prior to failure.

Figures 2 and 3 illustrate typical results from this series of tests. Figure 2 shows pore pressure ratio, $\Delta u/\bar{\sigma}_{vj}$, versus number of loading cycles, N , at various cyclic shear strain levels, for $D_r =$

38% and $\bar{\sigma}_{vj} = 204$ kPa. It is clear that the rate at which pore water pressure increases is higher for higher cyclic shear strain levels. The typical effect of relative density on pore water pressure accumulation is shown in Figure 3, wherein the pore water pressure buildup decreases as relative density increases. Figure 3 also indicates that for a given relative density and cyclic shear strain level, pore pressure ratio after a specific number of cycles decreases as initial effective vertical stress increases, although the differences are relatively minor. A similar effect was reported by Dobry, et al. (1982).

Figure 4 shows the effect of relative density and vertical stress on the number of cycles required to cause initial liquefaction, N_L . The symbols represent the averages from all tests. The figure indicates that N_L decreases as cyclic shear strain level increases, and that N_L increases for higher relative densities. Also, there is a slight trend for N_L to increase for higher initial effective vertical stresses at the same relative density.

The first series of tests involved no postliquefaction straining. Thus, volumetric reconsolidation strains measured in these tests should establish a baseline from which the effects of additional straining can be determined. Figure 5 shows the reconsolidation volumetric strains versus the cyclic shear strains for tests conducted at average relative densities of 38 and 80%, and $\bar{\sigma}_{vj} = 204$ kPa. It can be seen from Figure 5 that at a given relative density, the reconsolidation volumetric strain slightly increases as cyclic shear strain increases up to a shear strain of roughly 4%. However, if γ_{cy} is greater than 4%, the volumetric strain tends to remain constant, independent of the level of cyclic shear strain. Also, it is clear in Figure 5 that the reconsolidation volumetric strain depends on the relative density, with volumetric strain increasing as relative density decreases. Figure 6 shows the effect of initial vertical stress on the reconsolidation volumetric strains. Previous studies generally have indicated that vertical stress does not have a major effect on the magnitude of reconsolidation strains. Yet, there is a clear difference between the tests conducted at $\bar{\sigma}_{vj} = 54$ kPa and 204 kPa. It can be seen in Figure 6 that the reconsolidation volumetric strain increases by approximately one-third as initial effective vertical stress increased from 54 kPa to 204 kPa. Lee and Albaisa (1974) reported results of cyclic triaxial tests in which the volumetric reconsolidation strains were independent of initial effective confinement, $\bar{\sigma}_{ci}$, for pore pressure ratios, $\Delta u/\bar{\sigma}_{ci}$, less than about 0.6. For higher pore pressure ratios, the volumetric strains increased with increasing confinement, but were small, on the order of 0.8, 1.1, and 1.3% for effective confinements of 103, 207, and 414 kPa, respectively.

The effect of postliquefaction cycling on the volumetric strain due to reconsolidation was studied by bringing specimens to liquefaction at relatively small cyclic strains, γ_{cy-pre} , followed immediately by several cycles of large postliquefaction strains, $\gamma_{cy-post}$. Constant volume strain-controlled tests were performed at $D_r = 38\%$, $\bar{\sigma}_{vj} = 204$ kPa and preliquefaction cyclic shear strain levels of $\gamma_{cy-pre} = 0.1$ and 0.5%, as described before. After liquefaction, the specimens were cycled at constant postliquefaction cyclic shear strain amplitudes ranging from $\gamma_{cy-post} = 0.1$ to 15%. The number of postliquefaction cycles was kept constant at either $N_{post} = 10$ or 20.

The reconsolidation volumetric strains for specimens cycled up to liquefaction at $\gamma_{cy-pre} = 0.1$ and 0.5% with $N_{post} = 10$ are shown in Figure 7 as a function of the postliquefaction cyclic shear strains, $\gamma_{cy-post}$. It is clear that the volumetric strain does not depend on γ_{cy-pre} , when the

postliquefaction strains are larger than those causing liquefaction. The volumetric strains increase as $\gamma_{\text{cy-post}}$ increases up to about 4%. However, the volumetric strain remains constant as $\gamma_{\text{cy-post}}$ increases beyond 4%. The results of the tests cycled following liquefaction with $N_{\text{post}} = 10$ and 20 are presented in Figure 8. The figure reveals that the number of postliquefaction cycles does not influence the reconsolidation volumetric strains.

A comparison of the results of specimens reconsolidated immediately following liquefaction with the results of specimens reconsolidated after substantial postliquefaction cycling is shown in Figure 9. All the specimens had an average relative density of about 38% and were consolidated at $\bar{\sigma}_{\text{vi}} = 204$ kPa. The figure indicates that the results of the two types of tests are the same. Both sets of data indicate a slight increase in volumetric reconsolidation strains up to a shear strain of about 4%, after which there are no marked changes. Consequently, it can be concluded that the reconsolidation volumetric strain depends on the maximum cyclic shear strain experienced by the sand during the undrained cyclic loading, as long as liquefaction occurs.

As a follow up to the DSS testing at constant preliquefaction shear strain, a series of constant volume strain-controlled tests were carried out to study the effect of the wave form on the reconsolidation volumetric strain. After consolidation to $\bar{\sigma}_{\text{vi}} = 204$ kPa, specimens were cycled at constant shear strain level of 0.3% for five cycles. Then, specimens were cycled at a higher shear strain level ranging from 0.5 to 15% until initial liquefaction occurred. No postliquefaction cycles were applied. Volumetric strains due to reconsolidation after initial liquefaction were calculated and the results are presented in Figure 10, along with the results of tests in which a constant cyclic shear strain was applied until liquefaction occurred. The figure indicates that the volumetric strain is not affected by the wave form and depends on the maximum cyclic shear strain the sand experienced during undrained cycling.

Additional tests were conducted using the torsional shear (TS) device to confirm the trends found in the DSS tests. Specimens were consolidated isotropically to a confining pressure of $\bar{\sigma}_{\text{ci}} = 150$ kPa and $D_r = 38\%$. After initial consolidation, undrained cyclic strain-controlled tests were carried out at cyclic shear strain amplitudes ranging from 0.1 to 15%. No postliquefaction cycles were applied in these tests. Figure 11 compares the torsional shear and direct simple shear test results. The torsional shear results again indicate that the reconsolidation volumetric strain increases as cyclic shear strain increases up to 4%. Beyond $\gamma_{\text{cy}} = 4\%$, the volumetric strain remains constant, as concluded previously from the direct simple shear results.

COMPARISONS AND DISCUSSION

Several findings from the test results require discussion, in particular with respect to differences between trends presented elsewhere. The DSS test results indicated that the volumetric reconsolidation strains were dependent on the level of initial vertical stress, as reported by Lee and Albaisa (1974). Nagase and Ishihara (1988) studied the liquefaction characteristics of Fuji River sand in a torsional shear apparatus. The program involved irregular, stress-controlled, multidirectional shearing of saturated specimens. In that program, acceleration records from six earth-

quakes were converted to shear stress histories, and applied to the test specimens. The shear stress histories were scaled to cause varying levels of pore pressure ratio, $\Delta u/\bar{\sigma}_{ci}$, at the end of cycling. For tests in which the pore pressure ratios were less than one, the reconsolidation volumetric strains increased nearly linearly with increasing pore pressure ratios, and decreased with increasing relative density. These trends are consistent with those reported by others, and consistent with anticipated behavior. However, in the tests in which liquefaction ($\Delta u/\bar{\sigma}_{ci} = 1$) occurred, the measured volumetric strains were not defined uniquely as a function of pore pressure ratio. Nagase and Ishihara (1988) determined that the maximum shear strain, γ_{max} , that occurred at any point in the applied stress record could be used to determine the volumetric reconsolidation strain. This finding is significant, as it implies that reconsolidation strains are dependent on how the pore pressures are generated. In addition, they concluded that when the applied shear stress records were adjusted so that the irregular loading was just large enough to cause liquefaction, the maximum shear strain generated, γ_{max} , in all specimens was approximately 2.5 to 3.5% for relative densities in the range of approximately 50 to 90%. For specimens that did not liquefy prior to the complete application of the irregular loading, the maximum shear strains were less than that limit. Further analysis of the reconsolidation strains for all pore pressure ratios were found to be related directly to the maximum shear strain that occurred at any point in the tests. Ishihara and Yoshimine (1992) developed relationships between reconsolidation strains and maximum shear strains that were based on several important considerations. First, for situations in which liquefaction did not occur, volumetric strains could be related either to pore pressure ratio or cyclic strain. Secondly, liquefaction did not occur unless the cyclic shear strains during a test were at least equal to a threshold value of about 3%. Finally, volumetric strains at any relative density increased nearly linearly with maximum cyclic shear strain up to a second shear strain limit of about 8%, after which the volumetric strains remained constant.

Lee and Seed (1967) identify several ways in which failure in laboratory tests can be defined. One definition is when the zero effective stress condition develops, i.e., $\Delta u/\bar{\sigma}_{ci} = 1$. Another definition is based on a performance criterion in which strains reach some limiting value. A key difficulty with any definition based on a performance criterion such as a defined strain, is that there are many different strain levels that can be considered. Lee and Seed (1967) clearly showed that the strains at initial liquefaction decrease with increasing relative density, and that the onset of liquefaction in stress-controlled triaxial tests on loose sand specimens ($D_r = 38\%$) was accompanied by an immediate increase in the cyclic axial strains, ϵ_a , to approximately 10%. These trends in strain generation also were exhibited in stress-controlled cyclic simple shear tests (Peacock and Seed, 1968), wherein large strains ($\gamma \approx 15\%$) developed immediately following liquefaction in loose sands ($D_r = 50\%$). Furthermore, Lee and Albaisa (1974) presented test results from a loose sand ($D_r = 40\%$) that showed axial strains on the order of 10 to 14% when pore pressure ratios first become one, corresponding to a shear strain of $\gamma = 1.5$ $\epsilon_a = 15$ to 21%. Thus, establishment of a unique strain at failure in stress-controlled tests is difficult. There are, however, reasonable limits on the amount of strain that can be generated *in situ* during earthquakes, which are dependent on relative density, with maximum shear strains of about 35% at $D_r \approx 50\%$, and perhaps 5% for $D_r \approx 90\%$ (Seed, 1979). Such behavior is referred to as cyclic mobility with limited strain potential. Thus, the findings by Nagase and Ishihara (1988) identifying a unique level of shear strain, independent of relative density, with the condition of liquefaction represents a fundamentally new development in understanding stress-controlled testing

Nagase and Ishihara (1988) and Ishihara and Yoshimine (1992) have shown that reconsolidation volumetric strains are related uniquely to the maximum shear strain developed in the stress-controlled tests, up to strains of about 8%. Tatsuoka, et al. (1984) also investigated the effects of cyclic strain on reconsolidation volumetric strains. Those test results indicated increasing volumetric strains with increasing shear strains, but insufficient data were collected at cyclic shear strains greater than about 5%. Thus, a clear conclusion about a threshold strain limit cannot be drawn from that work, although there is some indication that the strain limit may be near 5%. Finn, et al. (1970) investigated the effects of strain history on the reliquefaction susceptibility of sand. Those tests included a series of strain-limited cyclic simple shear tests in which specimens were brought to liquefaction, and subjected to 15 cycles of shear strain prior to dissipation of the excess pore pressures. The specimens were then allowed to reconsolidate, and were tested again to determine any changes in cyclic strength that occurred as a result of the postliquefaction straining. The postliquefaction shear strains in tests performed by Finn, et al. ranged from $\gamma = 0.5$ to 11%. Thus, these tests are similar to those performed on the Nevada sand in this study. The tests conducted by Finn, et al. indicated that volumetric reconsolidation strains increased with the level of postliquefaction shear strain, for strains up to about $\gamma = 3\%$. However, for higher shear strains the volumetric strains remained nearly constant. The conclusion was drawn that above $\gamma = 3\%$, no further structural rearrangement of the soil skeleton occurs. This implies that cyclic strains following liquefaction in excess of $\gamma = 3\%$ may not lead to additional reconsolidation strain. This finding generally is consistent with the test results for the Nevada sand, although the Nevada sand showed a threshold strain of 4%.

Figure 12 presents reconsolidation volumetric strains measured by several groups, the design curves recommended by Ishihara and Yoshimine (1992), and the results from the Nevada sand tested at $\bar{\sigma}_{vj} = 204$ kPa. The design curves prepared by Ishihara and Yoshimine (1992) are based on many data generated by Nagase and Ishihara (1988), which are not shown on the figure. Figure 12 indicates a wide range in volumetric strains, and a general increase in volumetric strain for decreasing relative densities. However, the cyclic strain after which the volumetric strains tend to remain constant appears to be on the order of 3 to 5%. The results presented in Figure 12 show fundamental differences in interpreting stress-controlled and strain-controlled tests. Liquefaction can be induced in strain-controlled tests at low strain levels in only a few cycles. However, stress-controlled tests often define liquefaction failure as occurring at much higher strain levels (greater than 3%.)

The methods used most frequently in recent years for prediction liquefaction-induced settlements generally rely upon estimates of shear stress ratios generated by an earthquake and those causing liquefaction, as dependent on some index such as relative density or penetration resistance. (Tokimatsu and Seed, 1987; Ishihara and Yoshimine, 1992) Comparisons between measured and predicted settlements are in reasonable agreement, but are sensitive to the shear strain levels for very loose soil conditions.

Figure 13 presents a simple interpretation of the volumetric strains anticipated following liquefaction. The solid line in the figure represents the relationship given by the Tokimatsu and Seed (1987) design curves for volumetric strain for conditions in which liquefaction has occurred. The data shown on the figure are those from Japanese field observations from the 1968 Tokachioki

earthquake (Ohsaki, 1970), the 1964 Niigata earthquake (Building Research Institute, 1965), and the 1968 Miyagiken Oki earthquake (Tohno and Yasuda, 1981), as used by Tokimatsu and Seed to construct their design curves. Also shown on the figure are the results from this study on Nevada sand. The data from these tests on Nevada sand agree reasonably well with the others. As with the predictive method given by Tokimatsu and Seed (1987) and Ishihara and Yoshimine (1992), Figure 12 indicates that volumetric strains for site conditions having $(N_1)_{60}$ greater than about 30 are limited to about 1%. For sites where the soil is extremely loose, observed settlements may have been affected by other aspects of extensive liquefaction that make reliable measurements of actual ground settlements and back-calculated volumetric strains difficult. For many natural deposits, normal limits on relative densities often have a lower limit of 30 to 40%, with an upper limit on the order of 80%. Thus, it may be that typical maximum volumetric strains are limited to about 4%.

ACKNOWLEDGMENTS

The authors wish to thank the National Center for Earthquake Engineering Research (NCEER) which provided support under Grant No. 93-2301(S). The work of Ali Avcisoy in helping to prepare the figures is appreciated greatly

REFERENCES

- Arulmoli, K., K.K. Muraleetharan, M.M. Hossain, and L.S. Fruth (1991) "VELACS Verification of Liquefaction Analyses by Centrifuge Studies Laboratory Testing Program Preliminary Data Report," The Earth Technology Corporation, Sept.
- Building Research Institute (1965) "Niigata Earthquake and Damage to Reinforced Concrete Buildings in Niigata City," Report, Building Research Institute, Ministry of Construction, 43
- Dobry, R., R.S. Ladd, F.Y. Yokel, R.M. Chung, and D. Powell (1982) "Prediction of Pore Water Pressure Buildup and Liquefaction of Sands During Earthquakes by the Cyclic Strain Method," Building Science Series 138, National Bureau of Standards, Washington, D.C., July, 168 p.
- Finn, W.D.L., P.L. Bransby, and D.J. Pickering (1970) "Effect of Strain History on Liquefaction of Sand," Journal of the Soil Mechanics and Foundations Division, ASCE, Vol. 96, No. SM6, Nov., pp. 1917-1934.
- Ishihara, K. and M. Yoshimine (1992) "Evaluation of Settlements in Sand Deposits Following Liquefaction During Earthquakes," Soils and Foundations, JSSMFE, Vol. 32, No. 1, March, pp. 173-188.

Peacock, W.H. and H.B. Seed (1968) "Sand Liquefaction Under Cyclic Loading Simple Shear Conditions," Journal of the Soil Mechanics and Foundations Division, ASCE, Vol. 94, No. SM3, May, pp. 689-708.

Ladd, R.S. (1978) "Preparing Test Specimens Using Undercompaction," Geotechnical Testing Journal, ASTM, Vol. 1, No. 1, Mar, pp. 16-23.

Lee, K.L. and A. Albaisa (1974) "Earthquake Induced Settlements in Saturated Sands," Journal of the Geotechnical Engineering Division, ASCE, Vol. 100, No. GT4, Apr., pp. 387-406.

Nagase, H. and K. Ishihara (1988) "Liquefaction-Induced Compaction and Settlement of Sand During Earthquakes," Soils and Foundations, JSSMFE, Vol. 28, No. 1, March, pp. 65-76.

Ohsaki, Y. (1970) "Effects of Sand Compaction on Liquefaction During Tokachioki Earthquake," Soils and Foundations, JSSMFE, Vol. 10, No.2, pp. 112-128.

Pyke, R., H.B. Seed, and C.K. Chan (1975) "Settlement of Sand Under Multidirectional Shaking," Journal of the Geotechnical Engineering Division, ASCE, Vol. 101, No. GT4, Apr., pp. 379-398.

Seed, H.B. and M.L. Silver (1972) "Settlement of Dry Sands During Earthquakes," Journal of the Soil Mechanics and Foundations Division, ASCE, Vol. 98, No. SM4, Apr., pp. 381-397.

Seed, H.B. (1979) "Soil Liquefaction and Cyclic Mobility Evaluation for Level Ground During Earthquakes," Journal of the Geotechnical Engineering Division, ASCE, Vol. 105, No. GT2, Feb, pp. 201-255.

Silver, M.L. and H.B. Seed (1971) "Volume Changes in Sands During Cyclic Loading," Journal of the Soil Mechanics and Foundations Division, ASCE, Vol. 97, No. SM9, Sept., pp. 1171-1182.

Stewart, H.E. and A.K. Hussein (1992) "Determination of the Dynamic Shear Modulus of Holocene Bay Mud for Site-Response Analysis," The Loma Prieta, California, Earthquake of October 17, 1989 - Marina District, U.S. Geological Survey Professional Paper 1551-F, June, pp. F75-F83.

Tatsuoka, F., T. Sasaki, and S. Yamada (1984) "Settlement in Saturated Sand Induced by Cyclic Undrained Simple Shear," Proceedings, Eighth World Conference on Earthquake Engineering, San Francisco, Vol. III, pp. 95-102.

Tohno, I. and S. Yasuda (1981) "Liquefaction of the Ground During the 1978 Miyagiken-Oki Earthquake," Soils and Foundations, JSSMFE, Vol. 21, No. 2, pp. 18-34.

Tokimatsu, K. and H.B. Seed (1987) "Volume Changes in Sands During Cyclic Loading," Journal of Geotechnical Engineering, ASCE, Vol. 113, No. 8, Aug, pp. 861-878.

Yoshimi, Y., F. Kuwabara, and K. Tokimatsu (1975) "One-Dimensional Volume Change Characteristics of Sands Under Very Low Confining Stresses," Soils and Foundations, JSSMFE, Vol 15, No. 3, Sept., pp. 51-60.

Youd, T.L. (1972) "Compaction of Sands by Repeated Shear Straining," Journal of the Soil Mechanics and Foundations Division, ASCE, Vol. 98, No. SM7, July, pp. 709-725.

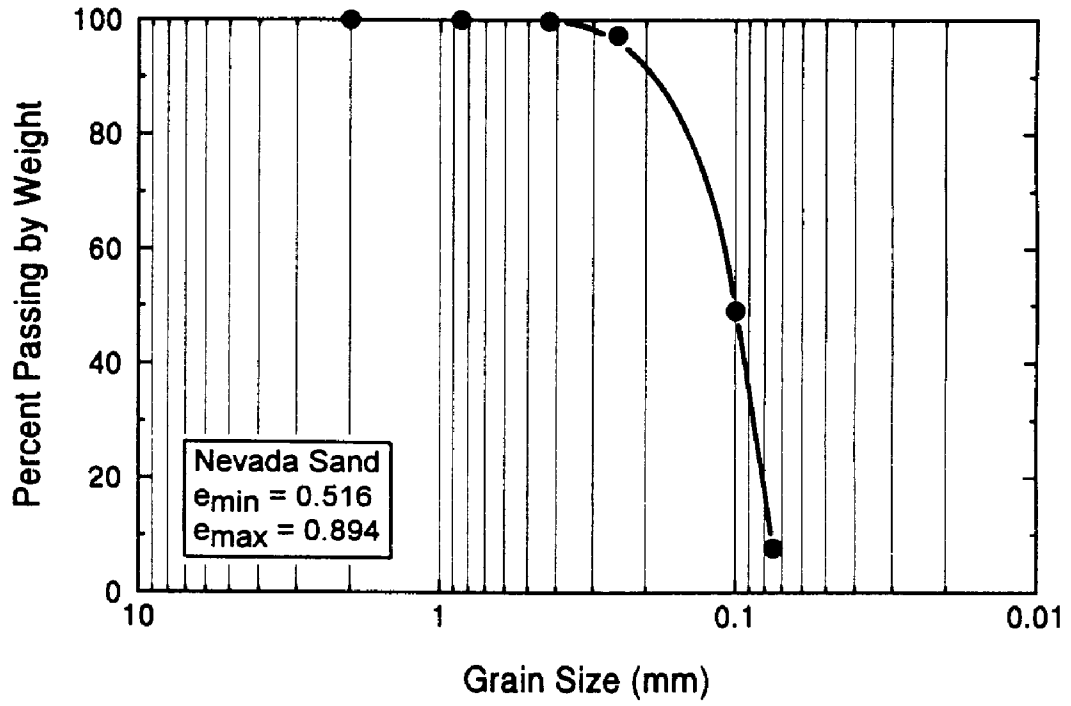


Figure 1. Grain Size Distribution Curve for Nevada Sand

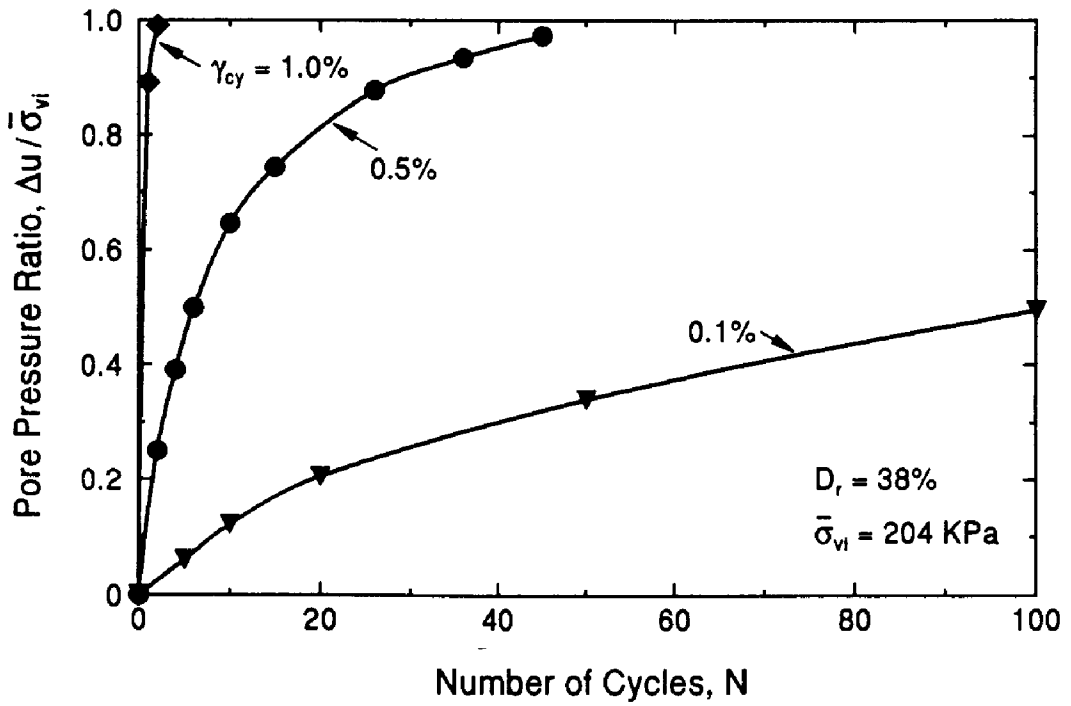


Figure 2. Pore Pressure Ratio versus Number of Cycles at Various Cyclic Shear Strain Levels

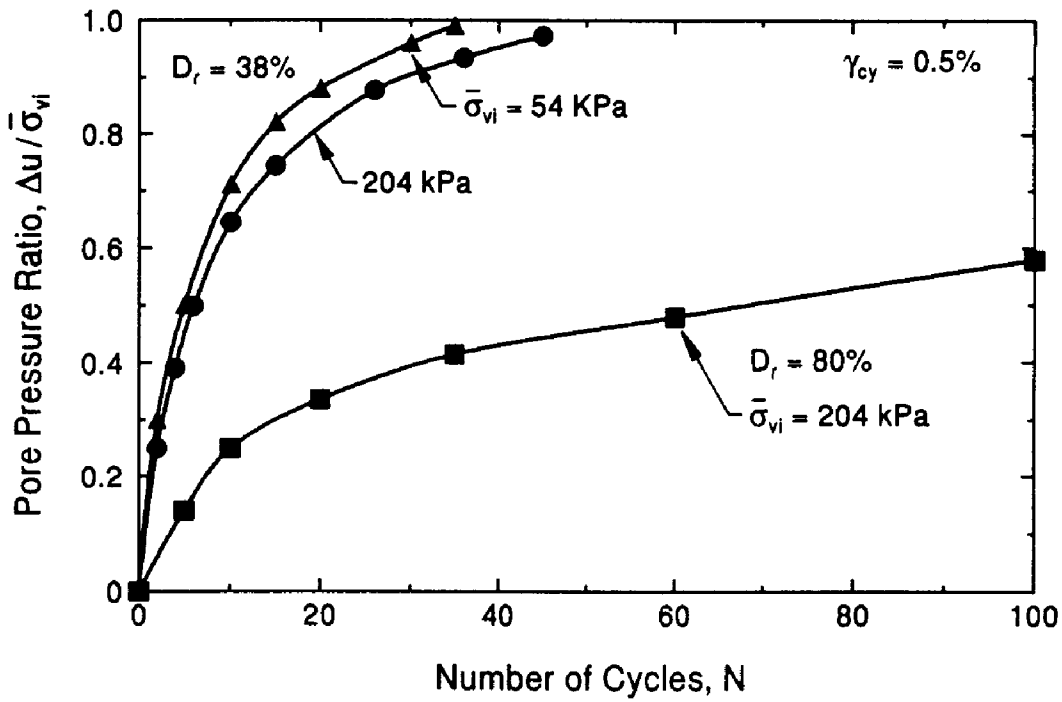


Figure 3 Effect of Relative Density and Initial Effective Stress on Pore Pressure Ratio

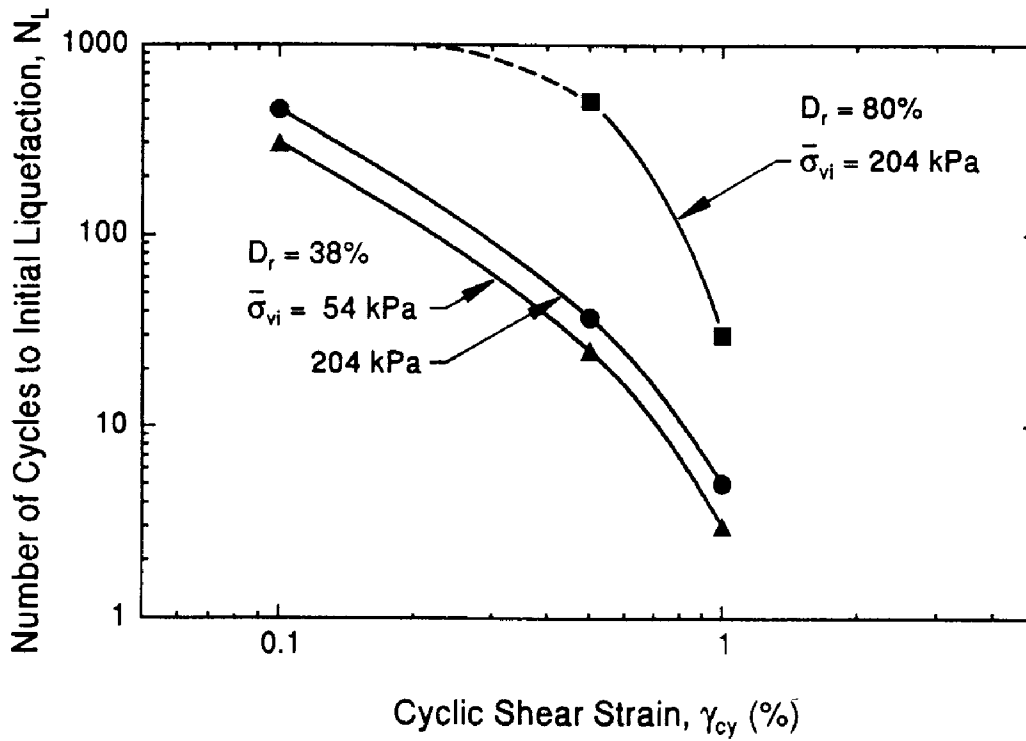


Figure 4 Effect of Relative Density and Initial Effective Stress on Number of Cycles to Liquefaction

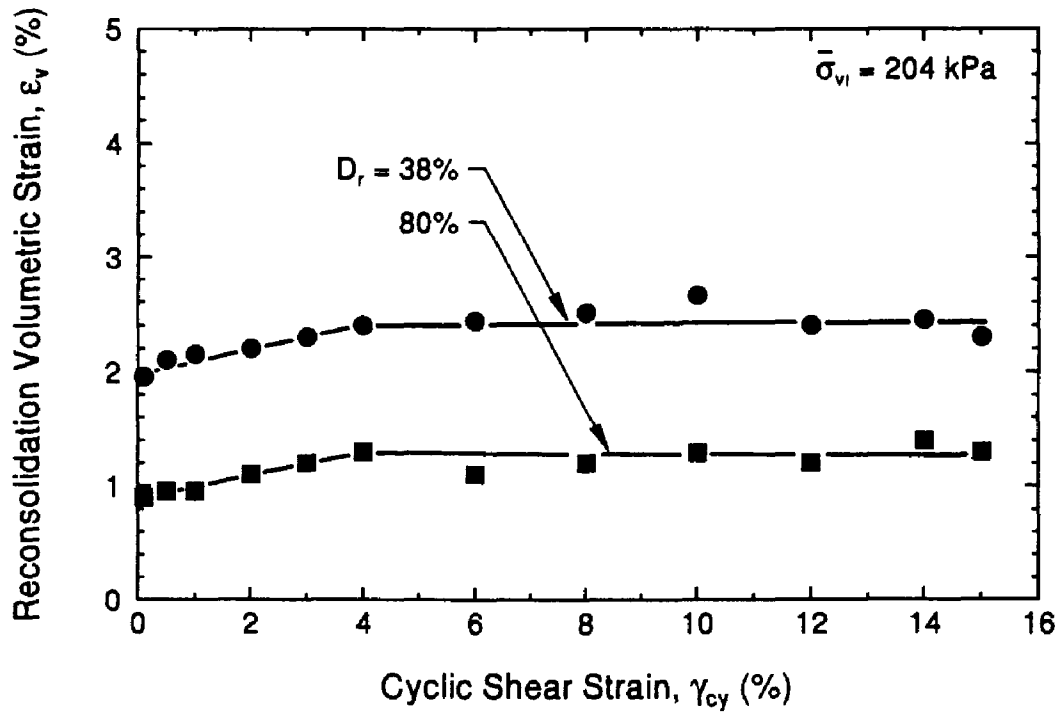


Figure 5. Effect of Relative Density on Reconsolidation Volumetric Strain

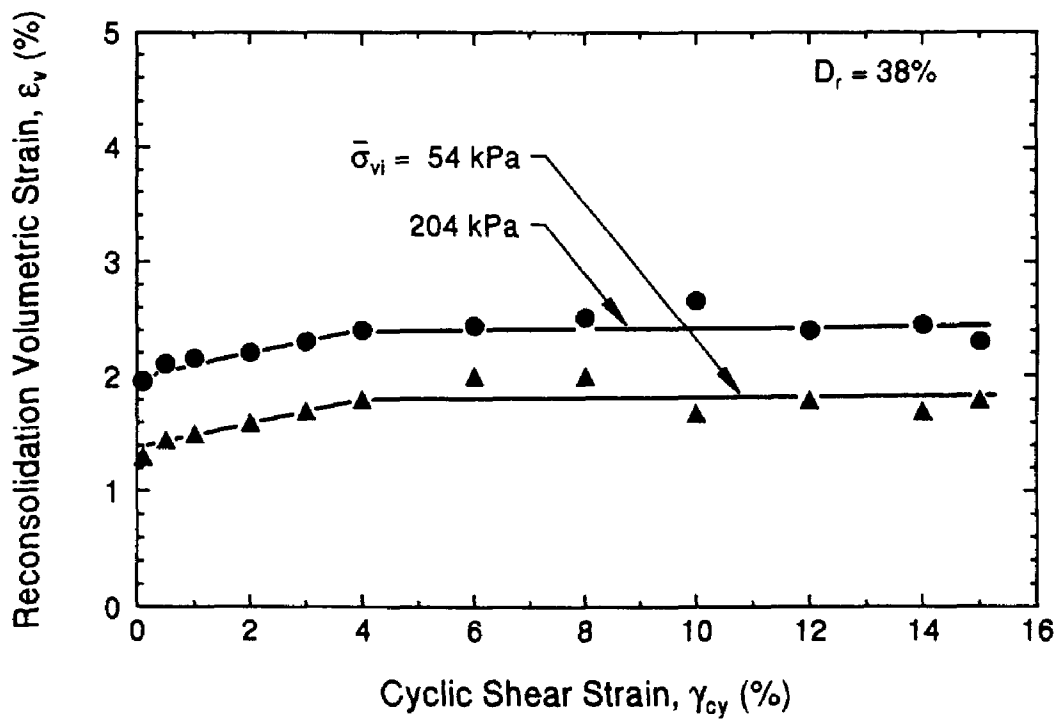


Figure 6 Effect of Initial Effective Stress on Reconsolidation Volumetric Strain

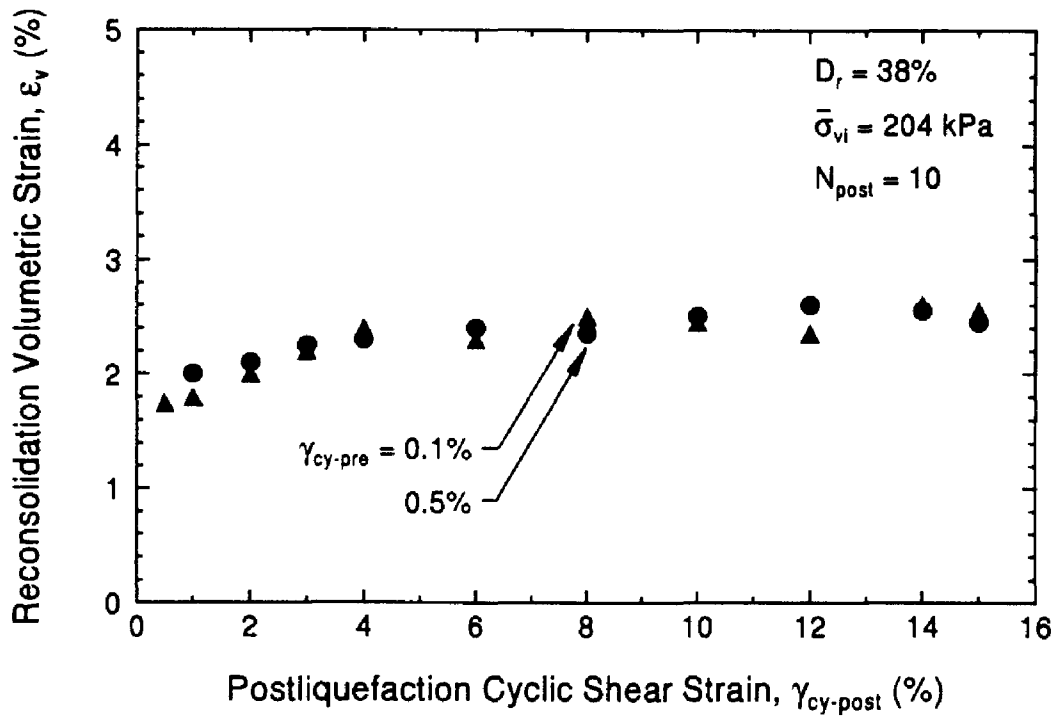


Figure 7 Effect of Postliquefaction Cycling on Reconsolidation Volumetric Strain

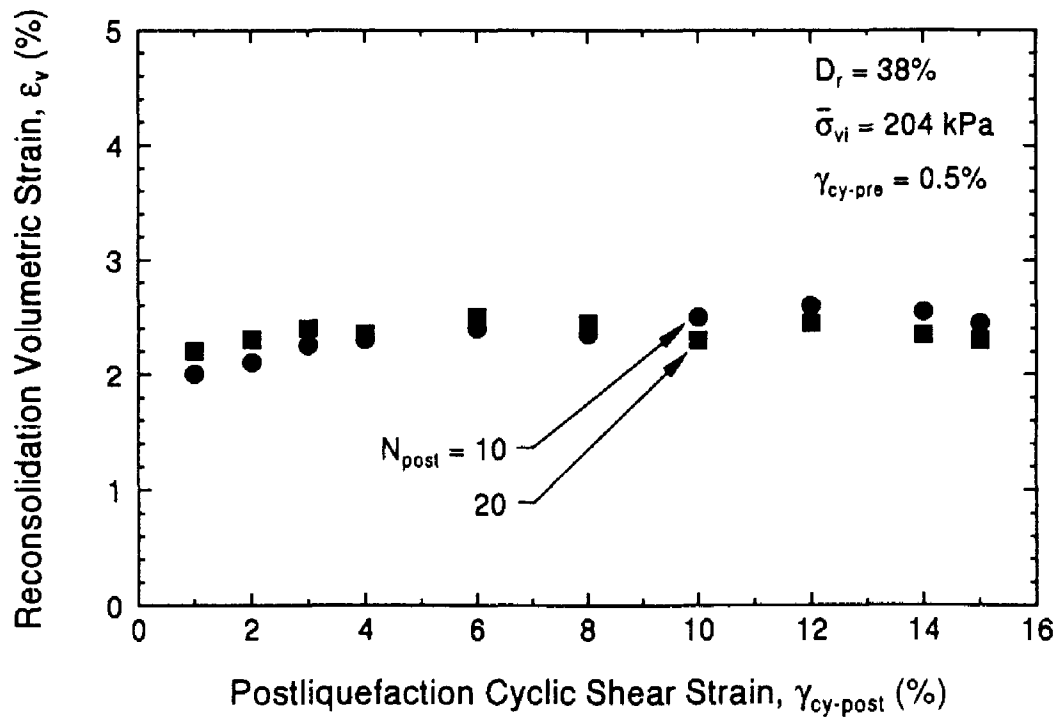


Figure 8 Reconsolidation Volumetric Strains for $N_{post} = 10$ and 20

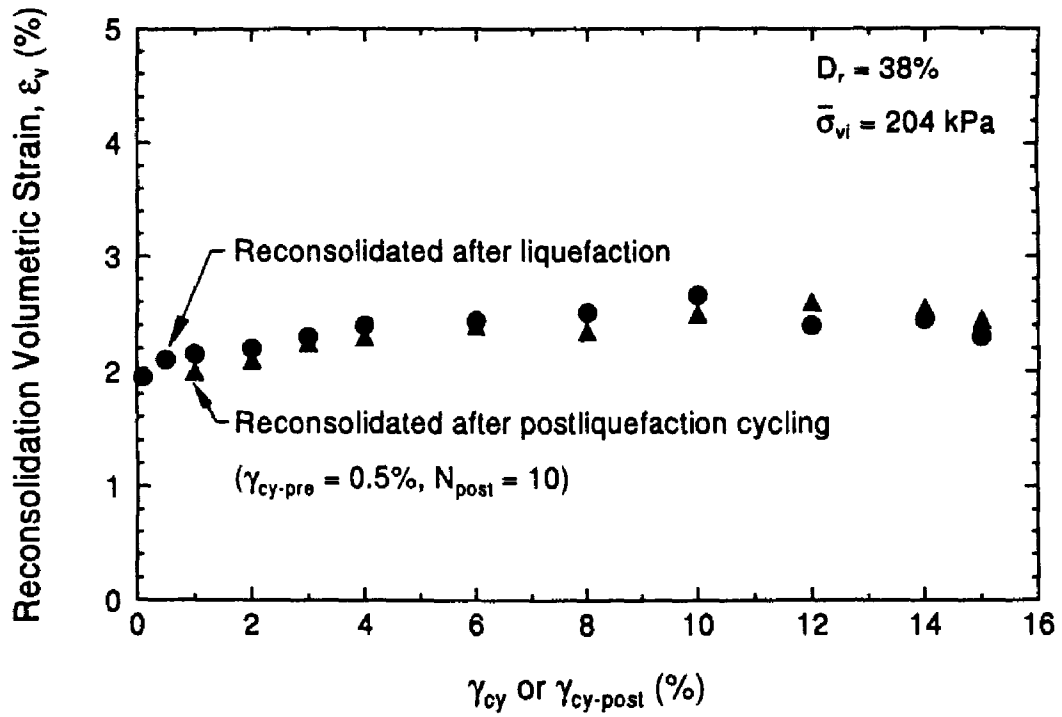


Figure 9. Comparison of Test Results with and without Postliquefaction Cycling

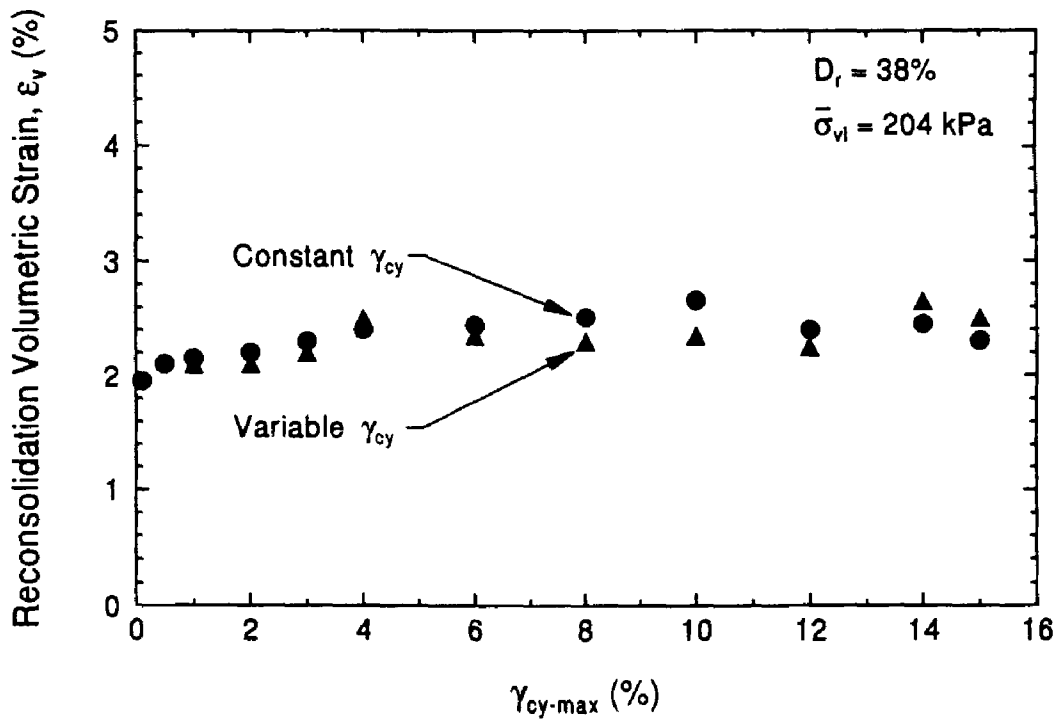


Figure 10 Reconsolidation Volumetric Strains for Different Wave Forms

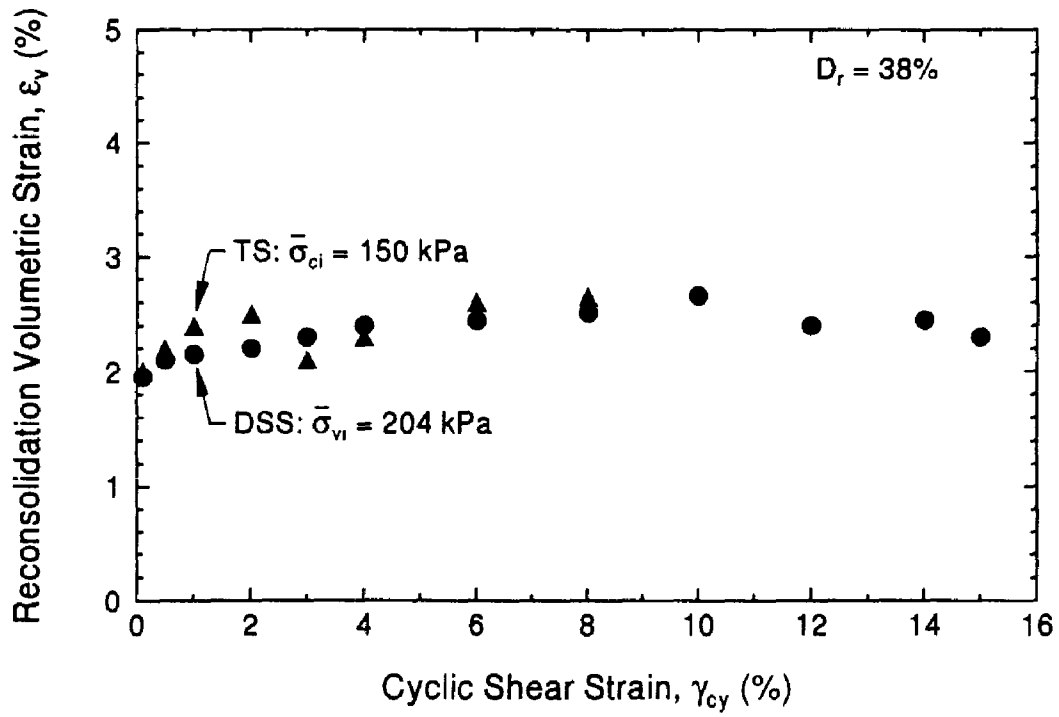


Figure 11. Comparison of Direct Simple Shear and Torsional Shear Tests Results

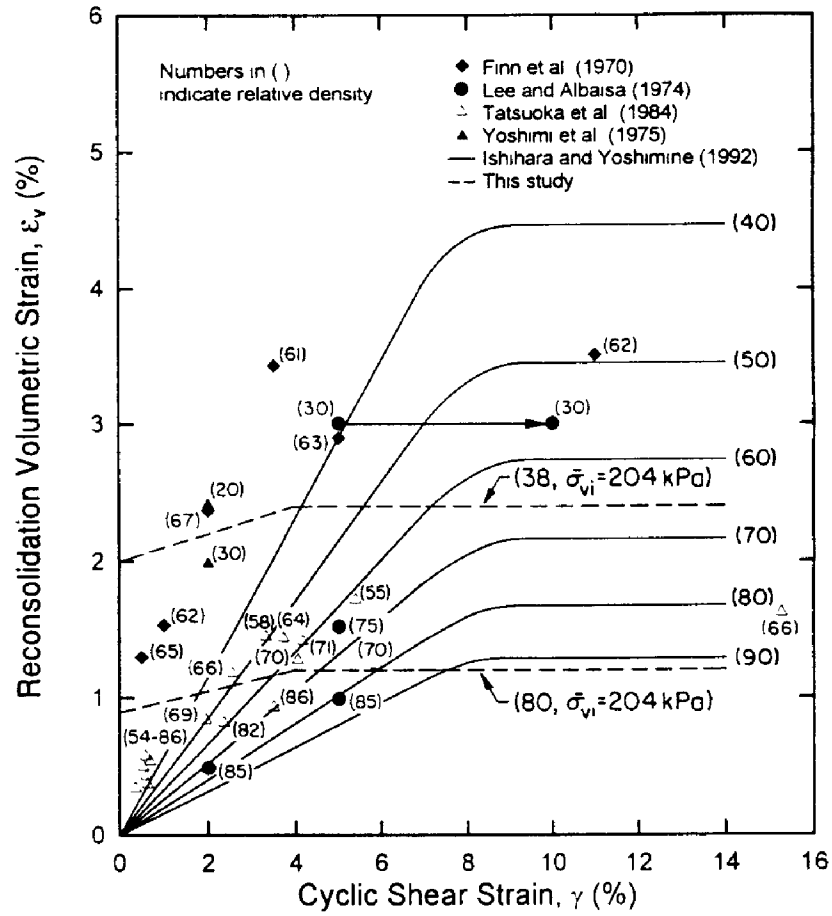


Figure 12 Reconsolidation Volumetric Strains from Various Studies

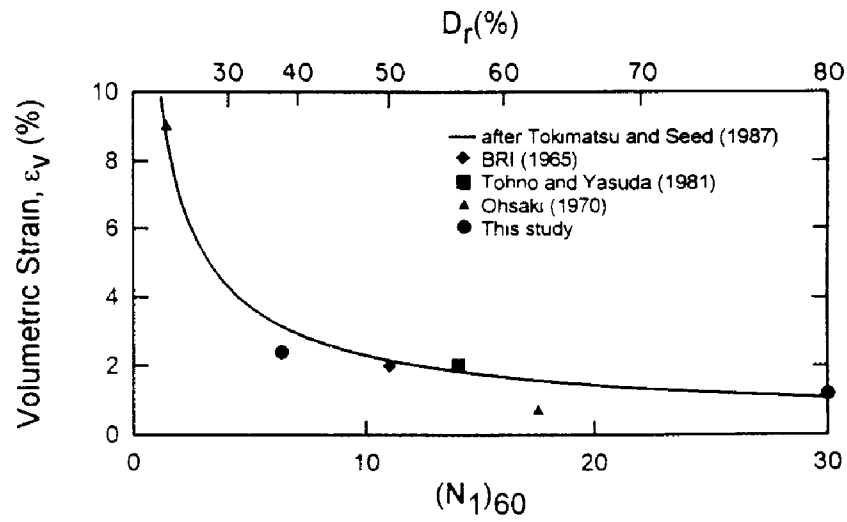


Figure 13 Simplified Curve for Estimating Reconsolidation Volumetric Strain